Title: Highly efficient Au hollow nanosphere catalyzed chemo-selective oxidation of alcohols

Author: Manickam Sasidharan Sundaramurthy
Anandhakumar Piyali Bhanja Asim Bhaumik

PII: S1381-1169(15)30110-2
DOI: http://dx.doi.org/doi:10.1016/j.molcata.2015.10.007
Reference: MOLCAA 9650

To appear in: *Journal of Molecular Catalysis A: Chemical*

Received date: 29-7-2015
Revised date: 5-10-2015
Accepted date: 6-10-2015

Please cite this article as: Manickam Sasidharan, Sundaramurthy Anandhakumar, Piyali Bhanja, Asim Bhaumik, Highly efficient Au hollow nanosphere catalyzed chemo-selective oxidation of alcohols, Journal of Molecular Catalysis A: Chemical http://dx.doi.org/10.1016/j.molcata.2015.10.007

Highly efficient Au hollow nanosphere catalyzed chemo-selective oxidation of alcohols

Manickam Sasidharan,[a*] Sundaramurthy Anandhakumar,[a] Piyali Bhanja[b] and Asim Bhaumik[b*]

[a]*SRM Research Institute, SRM University, Kattankulathur, Chennai, 603203, India,*

E-mail: sasidharan.m@res.srmuniv.ac.in

[b] *Department of Material Science, Indian Association for the Cultivation of Science, Jadavpur, Kolkata 700 032, India, E-mail: masb@iacs.res.in*

Graphical Abstract

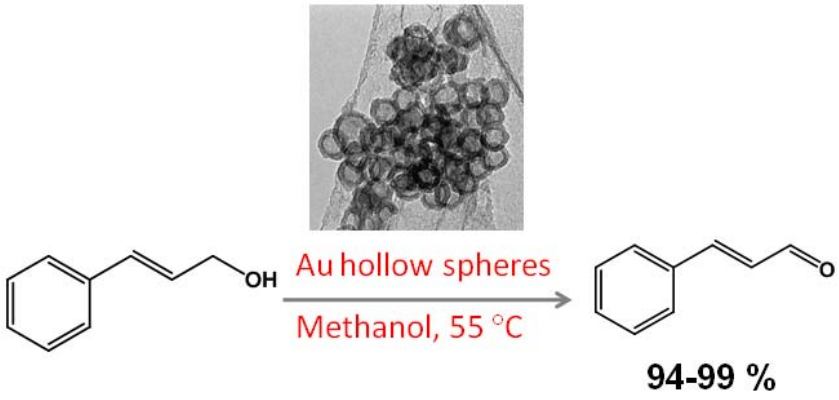

Hollow gold nanospheres of size less than 30 nm has been synthesized using triblock copolymer poly(styrene-*b*-2-vinyl pyridine-*b*-ethylene oxide) (PS-PVP-PEO) as a soft template and it showed excellent catalytic activity for the chemoselective oxidation of allylic unsaturated alcohols to the respective ketones in the presence of dilute aqueous H_2O_2 as an oxidant.

Research Highlights

1 First report of hollow Au nanospheres of size 26 ± 2 nm by soft-templating method.

2. Core-shell-corona type micelles of triblock co-polymer act as the template

3 Au hollow nanospheres exhibit excellent catalytic efficiency and chemoselectivity

4 Highly selective synthesis of carbonyl compounds under eco-friendly conditions.

ABSTRACT

Micelles of poly(styrene-*b*-2-vinyl pyridine-*b*-ethylene oxide) (PS-PVP-PEO) with *core-shell-corona* structures have been used as a scaffold for the fabrication of gold (Au) hollow nanospheres of particle size 26 ± 2 nm using $HAuCl_4$ and $NaBH_4$ as metal precursor and reducing agent, respectively. The PS *core* acts as a template for hollow void, the PVP *shell* serves as reaction sites for inorganic precursors, and PEO *corona* stabilizes the composite particles. Under acidic conditions, the PVP shell domain becomes positively charged pyridinum-species that electrostatically interacts with negatively charged $AuCl_4^-$ ions. On reduction of these composite particles and subsequent solvent extraction leads to the formation Au hollow nanospheres. Various analytical tools such as powder X-ray diffraction (XRD), transmission electron microscope (TEM), thermogravimetric analyses (TG/DTA), dynamic light scattering of (DLS) have been employed to characterize the polymeric micelles and hollow nanoparticles. The TEM and XRD studies confirmed the formation of highly crystalline Au hollow nanospheres. The Au hollow nanosphere/H_2O_2 system efficiently catalyzes the chemoselective oxidation of allylic-type unsaturated alcohols into aldehydes and ketones under mild liquid-phase conditions. The versatility of present catalytic system for the oxidation of other substrates like aliphatic-, acylic-, aromatic-, and heteroaromatic alcohols to their respective keto compounds has also been reported.

Keywords: Au hollow nanosphere, polymeric micelles, Au catalysts, chemoselective oxidation, oxidation of alcohols.

1. Introduction

Metal nanoparticles have been extensively investigated over the past two decades in many current and emerging areas of technology. Especially, monodispersed metal colloids of size less than 100 nm have found enormous potential application in areas including heterogeneous catalysis, solar photovoltaics, medicine, optics and electronics [1-9]. Noble metals in general, gold (Au) in particular, displays unique interesting features in many respects at the nanoscale level compared with micron-sized or bulk metals. For instance, nanometric particles exhibit surfaced Plasmon resonance due to interaction of electromagnetic waves confined electrons in nanomaterials [1]. In addition to composition and size, the shape/morphology is another important factor that determine the properties of nanoparticles. Advances in the synthesis of nanoparticles largely depend on the ability to synthesize materials of different sizes with interesting morphologies. Size control of Au nanoparticles were mainly accomplished by chemical strategies using various linear and star shaped poly(vinyl pyridine) macromolecules, biomass-derived compounds/polysaccharides, thiol ligands etc. as template or stabilizing agents [10-13]. Diblock copolymer PS-*b*-P2VP leads to the formation of micelles on dissolution in toluene comprising a P2VP core and a PS shell, which serves as an efficient soft-template to synthesize gold nanoparticles of size more than 10 nm by using metal salt and a reducing agent [14]. Whereas star-shaped PS-P2VP diblock copolymers effectively stabilize Au nanoparticles of size less than 5 nm during the synthesis in solution phase [15,16]. Thus the ability of block polymers to form stable micelles either in solution or at interfaces are main criteria for formation of gold nanoparticles with narrow particle size distribution and long term colloidal stability. Thus unlike the size-controlled growth, the field of morphology-controlled growth of Au nanoparticles is not well documented in the literature.

In a growing number of applications, the chemical composition and distribution of matter within the particles having unique morphology play important roles in determining a specific function. For example, the large fraction of void space in hollow structures has been used to modulate refractive index, increase active area for catalysis and drug delivery applications [17]. Hollow micro-/nanostructures of noble metals with void space in nano-metric dimension have been investigated in a variety of fields such as drug delivery, surface enhanced Raman scattering (SERS), sensors and catalysis [18-22]. On decreasing the dimension of metal particles, gold (Au) exhibits interesting properties that can be tuned to accomplish specific applications in nanotechnology. The well-known methods for synthesis of hollow nanospheres are to employ a suitable scaffold [23-27], such as polymer beads or emulsions to produce organic/inorganic composites materials, which upon calcination or solvent extraction provide spherical hollow particles. However this method leads to a broad particle size distribution and the homogeneity of the particles is often affected. To prepare monodispersed nanoparticles, self-assembled monolayer strategy using diblock polymers or biomoleucles [28-31] are also investigated with limited success. Li et al. have prepared Au spherical hollow particles of size about 100 nm through liposome mediated self-assembly of gold nanoparticles through reduction of $[(C_7H_{15})_4N]^+AuCl_4^-$ with EDOT (3,4-ethylenedioxy thiophene) as the reducing agent and TDPA (3,3'-thiodipropionic acid) as the stabilizing agents. The self-assembly of gold nanoparticles into hollow spherical particles is mainly facilitated by liposome formation in the preparation process [32]. In this context Gerthsen et al have fabricated gold hollow spheres of wall thickness of about 2-6 nm and inner diameter of 20-40 nm through a micro-emulsion technique [33].

Very recently, asymmetric triblock copolymeric micelles with *core-shell-corona* (CSC) architecture have been extensively investigated for fabrication of a variety of inorganic hollow

nanospheres with different compositions employing bottom-up chemistry approach [34-39]. The notable features and importance ABC triblock copolymers is that when dissolved in a suitable solvents, it forms CSC micelles having amphiphilic characters in such a way that *core* containing hydrophobic part acts as a template for void formation, the central hydrophilic *shell* domain serves as reaction site for reaction of inorganic metal precursors, and the hydrophilic *corona* block stabilizes the composite micelles. It is worth to mention at this juncture that although preparation of capped nanoparticles of size about 5 nm using stabilizing agents relatively easier than the fabrication of Au hollow nanospheres with similar wall thichkness, the presence of stabilizing agents in the former always encapsulates or binds with the metal surface to reduce free energy vis-à-vis number of binding sites but increase the colloidal stabilities than the latter, which is free from any stabilizing agents. Therefore, the motive of this investigation is to study the catalytic activity of uncapped bare Au surfaces of wall thickness of about 5-6 nm towards liquid phase oxidation reactions.

Since the pioneering work of Haruta et al. and others, for the low-temperature activation of CO by oxide-supported gold nanoparticles, heterogeneous catalysis based on gold nanoparticles has grown tremendously [40-43]. Recently, Tsukuda and co-workers have shown that gold nanoparticles dispersed in a support materials found to be an efficient aerobic oxidation catalysts [44,45]. On the other hand, low-dimensional Au nanoparticles effectively splits hydrogen molecules into atomic hydrogen, which is not observed at surfaces of bulk gold and hence, nano sized Au is of great importance for the development of new hydrogenation catalysts [46,47]. Thus metal hollow nanoparticles usually have high surface area to volume ratio vis-à-vis binding sites that ultimately governs catalytic activity in various organic transformations. The catalytic oxidative conversion of alcohols to their corresponding carbonyl compounds is one of

the fundamental processes for the production of fine chemicals and value added pharmaceutical intermediates [48-50]. In general, a base is necessary to activate the –OH groups thereby to achieve high yield and selectivity of desired carbonyl compounds; whereas the oxidation of alcohols under base-free conditions yields less targeted products. Recently, Corma *et al*. [51,52], Tsukuda et al [53] and Fan et al [54-56] reported that Au nano-clusters deposited on metal oxides or polymers are highly effective for aerobic oxidation of various alcohols in the absence of any base. Herein, we report a method for fabrication of uniform Au hollow nanospheres of size 26±2 nm templated by micelles of poly(styrene-*b*-vinyl-2-pyridine-*b*-ethylene oxide) (PS-PVP-PEO) using $HAuCl_4$ as metal source and sodium borohydride ($NaBH_4$) as a reducing agent under ambient conditions. The gold hollow nanoparticles are thoroughly characterized by XRD, TEM, FTIR, TG/DTA, DLS, and nitrogen sorption to confirm the morphology, crystallinity, phase purity and specific surface area. The Au hollow particles prepared by this method have been employed as an efficient heterogeneous catalyst for chemoselective oxidation of alcohols to the corresponding carbonyl compounds under liquid-phase conditions using dilute H_2O_2 as oxidant under base-free conditions.

2. Experimental

2.1 Preparation of polymeric micelles and gold hollow nanospheres

The micelle was first prepared by dissolving desired amount (100 mg) of PS(20.1k)-PVP(14.2k)-PEO(26k), (PS-PVP-PEO) in DMF containing 10 wt% water (For 0.1 g polymer, 4.5 g DMF and 0.5 water were used) and solubilized well by using a magnetic stirrer. The

DMF/H_2O solution was then dialyzed against water to obtain the micelles of PS-PVP-PEO free from DMF. The dialysis was carried out in a dialysis bag (30 cm length, 15 mm inner diameter) by immersing in a 500 mL capacity measuring jar containing about 300 mL water. It takes about 6 hours to attain equilibrium between DMF and H2O molecules and thereafter, the water was exchanged with fresh water. This process is repeated to about 10 to 12 times to ensure complete removal of DMF from the micelle inside the dialysis bag. Finally the concentrated micelle solution was transferred to 100 mL standard flask and diluted with water to obtain a polymer concentration 1 g/L. The pH of the aqueous micelle solution was adjusted to 4 using a dilute HCl (0.01M). Thus prepared micelle was further used for preparation of Au hollow nanospheres. In a typical synthesis, desired amount of micelle solution (polymer concentration of 1 g/L and pH 4) was taken in a conical flask and the micelle solution was constantly stirred using a magnetic stirrer. Then the desired amount of $HAuCl_4$ was added by keeping the molar ratio of $HAuCl_4$ to the pyridine unit of the PVP block at 15 (The molecular weight of PVP units in the above polymer 14,200 and molecular weight of 2-vinylpyridine (VP) unit 105; from this number of moles of VP can be calculated. The mixture was stirred for 2 days at room temperature (28-30 °C) followed by addition $NaBH_4$ solution ($NaBH_4/HAuCl_4$ = 3 in 1 mL H_2O) and further aged for 2 more days under static condition in an inert atmosphere. The polymer/metal composite particles were separated from the aqueous suspension by centrifugation (8000 rpm) and the solid was washed repeatedly with distilled water and ethanol to remove physisorbed polymeric materials. Finally, the hollow particles were obtained by solvent extraction with DMF under N_2 atmosphere.

2.2 Characterization

Powder X-ray diffraction (XRD) pattern was measured on a Rigaku RINT-2200 diffractometer with CuKα radiation (40kV, 30 mA) from 10 ° to 70 ° 2θ in 0.01 steps at a scan speed of 2°/min. BET surface area was measured by N_2 adsorption/desorption analysis at 77 K on a BELSORB 28SA analyzer after degassing of the sample at 150 °C for 3 h. Zetasizer Nano of Malvern Instruments was used to perform Dynamic light scattering (DLS) measurements. The correlation functions were analyzed by the cumulant method to determine the diffusion coefficient (*D)* of the micelles. The hydrodymamic diameter (D_h*)* was calculated from *D* using the Stokes-Einstein equation: $D_h - k_BT/3\pi\eta D$, where k_B is the Boltzmann constant, *T* the absolute temperature, and η the solvent viscosity. The transmission electron microscopic (TEM) images were recorded on a JEOL Electron Microscope operationg at 80 kV and 200 kV. In the case of micelle solutions, the TEM samples were prepared by casting a drop of micelle solution on a copper grid followed by staining with 1 wt% phosphotungstic acid, whereas for gold nanoparticles, a drop of aqueous suspension of the sample was coated on a copper grid. The samples were finally dried at room temperature. Thermogravimetric and differential thermograms (TG/DTA) were obtained with MAC Science TG-DTA 2100 under nitrogen. Fourier transform infrared (FTIR) spectra were recorded on Perkin Elmer spectrometer using KBr pellet technique. UV-visible spectra of gold nanoparticles were recorded with JASCO V-550 spectrometer using $BaSO_4$ as a reference.

2.3 Catalytic reaction

The liquid-phase oxidation reactions were performed using round bottom flask equipped with water condenser and a magnetic stirrer. In a typical alcohol oxidation reaction, 0.67 g (5

mmol) of cinnamyl alcohol was mixed with 5 mL of methanol and 0.56 g (5 mmol) of dilute H_2O_2 (30 wt% aqueous solution) in a 25 mL two-necked round bottom flask followed by addition of 5 wt% catalyst with respect to substrate. Cycloheptanone was used as an internal standard to quantify the reaction product. The reaction was performed at 328 K while effectively circulation ice-cold water through the condenser and the mixture was maintained under N_2 atmosphere using a N_2 balloon. The progress of the reaction was made by analyzing the products with a capillary gas chromatograph (Agilent 13G, OV-1 column with flame ionization detector, FID). The quantification of products has been performed with special care using internal standard and response factor of reactant and products. For catalyst reusability study, the catalyst was recovered through centrifugation followed by activation under 5 % H_2 (remaining N_2) atmosphere at 180 °C. It is pertinent to mention that low-temperature activation was carried out to remove the physically adsorbed organic reactant, product or solvent molecules from the metal surface of the used catalyst.

3. Results and discussion

3.1 Preparation of polymer micelles and Au hollow nanospheres

We have carried out the TEM analysis to confirm the spherical morphology PS-PVP-PEO polymeric micelles prior to its use as a soft template in the synthesis of Au hollow nanospheres. Further, light scattering experiments are employed to estimate average diameter of polymeric micelles. The estimated average diameter of PS-PVP-PEO micelles D_h (hydrodynamic diameter) is 61 nm at pH 4. It is well documented in the literature that the PS-PVP-PEO micelles

have a glassy and hydrophobic polystyrene core, a shell part consisting of ionizable hydrophilic polyvinyl pyridine units (PVP), and hydrophilic polyethylene oxide corona [57,58]. The notable feature of PVP units is that, it enlarges due to repulsive forces among the protonated PVP units on reducing the pH below 5. Fig. 1 shows the TEM image of the enlarged PS-PVP-PEO micelles stained with phosphotungstic acid. In individual spherical micelle image, the white contrast refers to the hydrophobic PS-core and the average diameter micelle particles estimated by TEM is found to be about 39 nm. The discrepancy in micelles particle's size values estimated from DLS and TEM is mainly due to exclusion of corona part in TEM observation. During hollow nanosphere synthesis, the addition of anionic species ($AuCl_4^-$) into PS-PVP-PEO micelle, electrostatic interaction prevails between anionic and cationic charge of the PVP unit, resulting in a size change in the PVP shell from an extended to a shrunken structure [59,60]. These features of structural change in PS-PVP-PEO micelle are investigated in the present method to deposit Au nanoparticles selectively on the shell domain of the micelles. The vinylpyridine functionality having cationic charges after protonation could electrostatically stabilize $AuCl_4^-$species in the shell domain, which is reduced subsequently to Au nanoparticles by the addition of $NaBH_4$. Scheme 1 depicts a general fabrication strategy for the formation of hollow gold nanospheres templated by PS-PVP-PEO micelles through electrostatic interaction followed by $NaBH_4$ reduction. At acidic pH, addition of $HAuCl_4$ to PS-PVP-PEO micelles leads to formation of $AuCl_4^-$ /polymer composite particles. On reduction with $NaBH_4$ under inert atmosphere, Au(III) is reduced to Au(0) in the shell domain, which upon solvent extraction with dimethylformamide (DMF) or toluene solvent leads to the formation of hollow nanospheres.

3.2 Characterization of Au hollow nanospheres

The TGA and DTA analyses (Fig. S1 and S2, supporting information) of the composite displayed a weight loss behavior in the temperature range from 25 to 900 °C. The weight loss below 100 °C could be attributed to the adsorbed water molecules, whereas the decomposition of PS-PVP-PEO polymer takes place at 405 °C. The strong electrostatic binding between cationic polyvinylpyridine units and negatively charged $AuCl_4^-$ species is the cause of high temperature degradation of polymeric materials. After solvent extraction of composite particles with DMF, the TG/DTA analyses suggested nearly complete removal of polymeric materials (Fig. S2, supporting information). The FTIR spectrum of Au/polymer composite particles also exhibits strong bands at 2864 and 2935 cm^{-1} corresponding to C–H stretching vibrations of alkyl groups of the polymer backbone (Fig. S3, supporting information). The band at 1360-1620 cm^{-1} is attributed to –C=C– bond stretching vibration of alkyl groups of the polymer backbone [61]. After solvent extraction of composite particles with DMF at 100 °C, these vibrational bands were completely disappeared due to removal of organic polymers from composite particles as suggested from the TG/DTA analyses. TEM image (Figure 2A) shows a monodispersed Au/polymer composite particles prior to extraction with DMF solvent and the average particle size was found to be 32 ± 2 nm. It is worthy to mention that, the average size of the Au/polymer composite particles was found to be lower than that of the spherical micelles particles (39 nm) determined prior to addition of $HAuCl_4$ precursors. Fig. S4 (supporting information) shows a UV-visible spectrum of colloidal gold hollow nanospheres in toluene and λ_{max} is observed around 528 nm, typically observed for red coloured gold colloids.

The TEM image of Au hollow nanospheres after solvent extraction and in the absence of any stabilizing agents is shown in Figure 2B. Similar to agglomeration of other nanoscale materials due to very high surface free energy and surface area, the Au hollow nanospheres also exhibit similar characteristics of aggregation in the absence of stabilizing agents to a certain extent, which increases as the particle size decreases. Furthermore, two or more spherical particles also combines to produce either a large hollow spherical particles or a nanotube like structure with end-capped as seen from Fig. 2B. The specific features of hollow gold particles including particle diameter, hollow cavity size, and wall thickness were estimated from the TEM picture. To estimate average particle size and void space, we picked up about 100 spherical particles (Fig. S5, supporting information) and the calculated average particle size was 26 ± 2 nm and void-space diameter was found to be 16 ± 1 nm. The wall thickness estimated from TEM was about 5 ± 0.5 nm. Furthermore, size distribution estimated through DLS studies (Fig. S6, supporting information) suggested a narrow particle size distribution of 30–34 nm. The observed slightly higher average particle size in DLS experiment is presumably due to aggregation in the presence of solvent. Figure 2C exhibits high-resolution transmission electron microscopic (HRTEM) image, indicating lattice fringes originating from a Au nanocrystals and the lattice spacing of 0.24 nm which corresponds to (111) plane (0.2355 nm) for fcc bulk Au [62]. The electron diffraction (ED) pattern of gold nanoparticles also clearly confirm very high crystallinity from observed (111), (200), (220), (311), and (222) diffractions of face-centered cubic phase of metallic gold (Figure 2D) [63]. Energy dispersive X-ray analysis (Fig. S7, supporting information) further suggests that the nanoparticles are phase pure and no amorphous impurities are present. An XRD pattern of Au hollow nanospheres recorded in the range of 30 - 70° 2θ is shown in Figure 3. The diffraction peaks were observed at 38.1°, 44.4°, and 64.8°, which

corresponds to the (111), (200), and (220) planes of the fcc bulk Au particles, respectively. The combination of TEM and XRD results clearly confirm the crystallinity and phase purity of gold hollow nanospheres. The N_2 adsorption/desorption analysis of Au NPs at liquid-nitrogen temperature (77 K) displayed steady increase in N_2 uptake in the intermediate region of P/P_0 together with a mild hysteresis loop (Fig. S8, supporting information). This N_2 sorption analysis suggested the BET surface area of 47 m^2g^{-1} for the hollow gold nanoparticles (Fig. S9, supporting information). These Au hollow nanospheres with high BET surface area have been employed for the selective oxidation of alcohols under liquid-phase conditions using dilute aqueous H_2O_2 as oxidant.

3.3 Influence of solvents over different solvents using Au hollow nanospheres/H_2O_2

Chemoselective oxidation of a specific functional group in presence of other functionalities is an important fundamental oxidative transformation in organic synthesis. Recently, we have reported region-selective epoxidation of olefins containing different C=C bonds such as terminal- and internal-double bonds using Ti-β as solid-heterogeneous catalysts under mild conditions [64]. In the partial oxidation chemistry, enormous research effort has been focused towards chemoselective oxidation of alcohols with heterogeneous solid catalyst under mild liquid-phase conditions. In spite of significant growth in catalysts development, only very few catalysts capable of activating nonactivated alcohols such as aliphatic- and alicyclic-alcohols and strong bases such as KOH or K_2CO_3 are needed to promote the oxidation of primary aliphatic alcohols [65-67]. However, in the current study no base is used and we presume that Au nanocatalyst activates the −O−H bonds in the substrates efficientl,y thereby eliminates the

requirement of an additional base. The nature of different solvents over the activity and selectivity of oxidized products using Au nanosphere/H_2O_2 catalytic system is shown in Table 1. The chemoselective oxidation of cinnamyl alcohol is performed (Scheme 2) as a standard reaction to study the influence of solvents with different polarities and basicities using Au/H_2O_2 system. As shown in Table 1, the use of mild-basic acetonitrile (entry 1) leads to smooth oxidation product but the protic-polar solvents such as methanol and ethanol exhibit marginally higher reactivity of cinnamyl alcohol as well as desired product selectivity (entries 2 and 3) than acetonitrile solvent. The Au-hollow nanoparticles due to its nano-size and high-surface area vis-à-vis binding sites effectively adsorb alcohol-reactants to provide the corresponding ketones in high yield. Although the activity in dichloromethane (entry 4) is moderate, it provides better selectivity for required carbonyl compound. The solvents nitromethane and ethylacetate (entries 5 and 6) also exhibited a high reactivity with marginally decreased product selectivities. The non-polar solvent toluene (entry 7) shows relatively lower reactivity as well as product selectivity than the polar solvents (entries 2 and 3). Among the various solvents scrutinized, the highest activities and product selectivities are observed for the methanol solvent. Therefore, methanol is chosen as solvent for the subsequent catalytic reactions over different substrates under similar reaction conditions. The critical amount of catalyst required for optimal reaction is also evaluated by carrying out the oxidation reaction with different catalyst loading (entries 1, 8, and 9) and when the Au-nanoparticles loading is decreased to 3% from 5%, the conversion of cinnamyl alcohol decreases to nearly 20 % and hence, 5 wt% catalyst is used for further studies.

3.4 Reactivity of different substrates using Au hollow nanospheres/H_2O_2

Under optimized reaction conditions, we focused our attention to a wide range of alcohols. The chemoselective oxidation of various cyclic and aliphatic unsaturated alcohols over Au-nanoparticles/H_2O_2 catalytic system showed good yields for the desired products (Table 2). The selective oxidation of both cyclic and acyclic alcohols proceeded smoothly to give corresponding aldehyde or ketones in high yields. Both primary and secondary alcohols with "allylic structure" gave corresponding aldehyde and ketones, respectively (entries 1 and 2). Notably, Au-nanospheres/H_2O_2 is found to catalyze the oxidation of various unactivated alcohol like 1-hexene-1-ol and nonene-1-ol with very high conversion as well as product selectivity (entries 3-5). In addition, the scope of present catalytic system has also been investigated over various activated, and heteroatom containing alcohols. 1-pyridine ethanol containing nitrogen atom (entry 6) oxidizes to the corresponding ketone with 99 % selectivity. The ring activated benzylic substrates (entries 7-9) lead to near complete conversion but yields mixture of products comprised of carboxylic acid and aldehydes; whereas unactivated 4-bromo benzylic substrate (entry 10) gave moderate yield due high electronegativity of bromide groups. The cyclic alcohol and unactivated aliphatic alcohols (entries 11 and 12) also get converted into the corresponding carbonyl compounds in good yields. The alcohol oxidation is also performed in the absence of Au-nanospheres using H_2O_2 under similar conditions, where only traces of cinnamaldehyde is produced (entry 13). The Au-nanospheres are separated by centrifugation, washed thoroughly with ethanol followed activation at 180 °C using 5 % H_2 diluted with N_2 gas. We have recycled the liquid phase oxidation reaction four times by using the same Au nanocatalyst and no significant loss of catalytic activity is observed (entry 14, Fig. S10, supporting information). More interestingly, the spherical and hollow particle morphology of the sample is almost retained (Fig. S11, supporting information). Further to confirm the true heterogeneous nature of

Au catalyst, the leaching test has been carried out after 6 h at 328 K, followed by hot filtration to remove catalysts (Table S1, supporting information). Then the reaction mixture is magnetically stirred for a period of another 6 h in absence of any catalyst under similar experimental conditions. Analysis of the reaction mixture after 6 h showed neither increase in reactant conversion nor any side reactions suggesting that leaching of Au did not take place during the reaction and also confirms heterogeneous nature of present catalytic system.

Furthermore, for comparison solid Au spherical nanoparticles of dimension 20-30 nm have been synthesized via citrate reduction method [68] and their morphology has been analyzed by TEM (Fig.S12, supporting information). This Au nanosphere is used as the catalyst for the oxidation of cinnamyl alcohol and only 72.9 conversion is observed under similar conditions (entry 15). It is important to note that Au nanoparticles of size less than 10 nm should be stabilized by a stabilizing or capping agent, since nanoparticles have very high free energy and tend to undergo aggregation. As the smaller particle's surface is masked or encapsulated by organic molecules, the relative number of binding sites available for chemical reactions is lower than that available for the uncapped hollow nanoparticles. Here the surface of the Au hollow particles is bare and large number binding sites are available both at internal and external surface of the hollow nanospheres for carrying out the organic reactions. Further, considering the gold density 19.3 gcm^3 and the Au NPs spherical geometry (r = 13.0 nm), the expected theoretical specific surface area for solid Au nanospheres of similar dimension would have been 11.9 m^2g^{-1}. Whereas, Au hollow nanospheres synthesized by using PS-PVP-PEO polymeric micelles have the BET surface area of 47 m^2g^{-1}. This inter-nanosphere void surface could be responsible for the higher catalytic activity of our Au hollow nanospheres over solid Au nanospheres of similar dimension. Regarding reaction mechanism, it is believed that the α-hydrogen abstraction of an

alcohol may be involved in the rate determining step based on the isotope kinetic study (K_H/K_D = 1.7-2.0) [69]. According to Fan *et al*. [70] the key aspect of H_2O_2 is to facilitate the abstraction of the α-hydrogen as a hydrogen scavenger leading to the formation Au-alcoholate complex, which is further attacked by H_2O_2 to form the final carbonyl compound *via* β-elimination pathway. Based on these literature reports we firmly believe that the present catalytic system would follow similar mechanistic pathway in the selective oxidation of alcohols to ketones in the presence of dilute aqueous H_2O_2 as oxidant.

4. Conclusion

The *core-shell-corona* micelle-templating strategy using ABC triblock copolymer PS-PVP-PEO has been successfully employed to synthesize monodispersed Au hollow nanospheres of size 26±2 nm under very mild reaction conditions. High resolution TEM, electron diffraction pattern, and X-ray diffraction results confirmed the hollow nanosphere morphology of the Au nanoparticles and good crystallinity. FTIR spectroscopic analyses suggested that solvent extraction using DMF effectively removes polymeric templates from composite particles to obtain Au hollow nanospheres. The Au hollow nanospheres serve as an efficient heterogeneous reuable catalyst for selective oxidations for a variety of unactivated/activated cyclic as well as acylic alcohols to the corresponding carbonyl compounds. The catalysts exhibit remarkable reusability and excellent efficiency for repeated reuses, suggesting a huge potential of monodispersed Au hollow nanospheres in eco-friendly liquid phase oxidation catalysis in future.

Acknowledgements.

MS thanks Science and Engineering Research Board for financial support (SB/S1/PC-043/2013). PB thanks CSIR, New Delhi for a Junior Research Fellowship. AB thanks DST, New Delhi for providing DST-SERB project grant.

References

[1] M. C. Daniel, D. Astruc, Chem. Rev. 104 (2004) 293-346

[2] M. D. Hughes, Y.-J. Xu, P. Jenkins, P. McMorn, P. Landon, D. I. Enache, A. F. Carley, A. G. Attard, G. J. Hutchings, F. King, E. H. Stitt, P. Johnston, K. Griffin, C. J. Kiely, Nature 437 (2005) 1132-1135.

[3] T. Ishida, M. Haruta, Angew. Chem. Int. Ed. 46 (2007) 7154-7156.

[4] A. Corma, H. Garcia, Chem. Soc. Rev. 37 (2008) 2096-2126.

[5] J. Zeng, Q. Zhang, J. Y. Chen, Y. N. Xia, Nano Lett. 10 (2010) 30-35.

[6] C. H. Campos, M. Jofre, C. C. Torres, B. Pawelec, J. L. G. Fierro, P. Reyes, Appl. Catal. A: Gen. 482 (2014) 127-136

[7] T. Sun, Y. S. Zhang, B. Pang, D. C. Hyun, M. Yang, Y. Xia, Angew. Chem. Int. Ed. 53 (2014) 12320-12364.

[8] N. Li, P. X. Zhao, D. Astruc, Angew. Chem. Int. Ed. 53 (2014) 1756-1789

[9] J. J. Martinez, H. Rojas, L. Vargas, C. Parra, M. H. Brijaldo, F. B. Passos, J. Mol. Catal. A: Chem. 383 (2014) 31-37.

[10] M. B. Dickerson, K. H. Sandhage, R. R. Naik, Chem. Rev. 108 (2008) 4935-4978.

[11] E. Kharlampieva, V. Kozlovskaya, O. Zavgorodnya, G. D. Lilly, N. A. Kotov, V. V. Tsukruk, Soft Matter. 6 (2010) 800-807.

[12] R. A. D. Arancon, S. H. T. Lin, G. Chen, C. S. K. Lin, J. P. Lai, G. B. Xu, R. Luque, RSC Adv. 4 (2014) 17114-17119.

[13] J. Sun, H. X. Wu, Y. D. Jin, Nanoscale 6 (2014) 5449-5457

[14] J. P. Spatz, S. Mossmer, C. Hartmann, M. Moller, T. Herzog, M. Krieger, H. G. Boyen, P. Ziemann, Langmuir 16 (2000) 407-415

[15] J. H. Youk, M. K. Park, J. Locklin, R. Advincula, J. Yang, J. Mays, Langmuir 18 (2002) 2455-2475

[16] M. Filali, M. A. R. Meier, U. S. Schubert, J. F. Gohy, Langmuir 21 (2005) 7995-8000

[17] X. W. Lou, L. A. Archer, Z. Yang, Adv. Mater. 20 (2008) 3987-4019

[18] F. Caruso, Adv. Mater. 13 (2001) 11-22.

[19] M. A. El-Sayed, Acc. Chem. Res. 34 (2001) 257-264.

[20] Y. C. Cao, R. Jin, C. A. Mirkin, Science 297 (2002) 1536 – 1540.

[21] R. Narayanan, M. A. El-Sayed, Nano Lett. 4 (2004) 1343-1348.

[22] P. G. S. Abadi, E. Rafiee, S. Nadri, G. Hajian, M. Joshaghani, Appl. Catal. A: Gen. 487 (2014) 139-147

[23] Z. Zhong, Y. Yin, B. Gates, Y. Xia, Adv. Mater. 12 (2000) 206-209.

[24] I. Santos, B. Scholer, F. Caruso, Adv. Funct. Mater. 11 (2001) 122-128.

[25] F. Caruso, M. Spasova, V. S. Maceira, M. L. Marzan, Adv. Mater. 13 (2001) 1090-1094.

[26] G. H. Wang, J. Hilgert, F. H. Richter, F. Wang, H. J. Bongard, B. Spliethoff, C. Weidenthaler, F. Schueth, Nat. Mater. 13 (2014) 294-301.

[27] J. P. Han, G. Y. Xu, B. Ding, J. Pan, H. Dou, D. R. MacFarlane, J. Mater. Chem. A 2 (2014) 5352-5357.

[28] B. Putlitz, K. Landfester, K. Fisher, M. Antonietti, Adv. Mater. 13 (2001) 500-503

[29] L. Zhang, A. Eiserberg, J. Am. Chem. Soc. 118 (1996) 3168-3181.

[30] J. H. Fuhrhop, W. Helfrich, Chem. Rev. 93 (1993) 1565-1582.

[31] D. H. W. Hubert, M. Jung, A. L. German, Adv. Mater. 12 (2000) 1291-1294.

[32] X. Li, Y. Li, C. Yang, Y. Li, Langmuir 20 (2004) 3734-3739.

[33] C. Zimmermann, C. Feldmann, M. Wanner, D. Gerthsen, Small 3 (2007) 1347-1349.
[34] A. Khanal, Y. Inoue, M. Yada K. Nakashima, J. Am. Chem. Soc. 129 (2007) 1534-1535.
[35] M. Sasidharan, K. Nakashima, Acc. Chem. Res. 47 (2014) 157-167
[36] M. Sasidharan, K. Nakashima, N. Gunawardhana, T. Yokoi, M. Inoue, S. Yusa, M. Yoshio, T. Tatsumi, Chem. Commun. 47 (2011) 6921-6923.
[37] S. K. Das, M. K. Bhunia, D. Chakraborty, A. R. Khuda-Bukhsh, A. Bhaumik, Chem. Commun. 48 (2012) 2891-2893.
[38] M. Sasidharan, N. Gunawardhana, M. Inoue, S. Yusa, M. Yoshio, K. Nakashima, Chem. Commun. 48 (2012) 3200-3202
[39] M. Sasidharan, H. Zenibana, M. Nandi, A. Bhaumik, K. Nakashima, Dalton Trans. 42 (2013) 13381-13389
[40] M. Haruta, T. Kobayashi, H. Sano, and N. Yamada, Chem. Lett. (1987) 405-408.
[41] B. J. Borah, S. J. Borah, K. Saikia, D. K. Dutta, Catal. Sci. Technol. 4 (2014) 4001-4009
[42] N. T. Khoa; S. W. Kim, D. H. Yoo, E. J. Kim, S. H. Hahn, Appl. Catal. A: Gen. 469 (2014) 159-164.
[43] E. Rombi, M. G. Cutrufello, R. Monaci, C. Cannas, D. Gazzoli, B. Onida, M. Pavani, I. Ferino, J. Mol. Catal. A: Chem. 404 (2014) 83-91.
[44] H. Tsunoyama, N. Ichikuni, H. Sakurai, T. Tsukuda, J. Am. Chem. Soc. 131 (2009) 7086-7093.
[45] Y. Y. Fang, Y. Z. Chen, X. Z. Li, X. C. Zhou, J. Li, W. J. Tang, J. W. Huang, J. Jin, J. T. Ma, J. Mol. Catal. A: Chem. 392 (2014) 16-21
[46] P. Claus, Appl. Catal. A 291 (2005) 222-229.
[47] C. Kartusch, J. A. van Bokhoven, Gold Bull. 42 (2009) 343-348
[48] R. A. Sheldon, J. K. Kochi, Metal-Catalyzed Oxidation of Organic Compounds, Academic Press, New York, 1981.
[49] S. Verma, M. Nandi, A. Modak, S. L. Jain, A. Bhaumik, Adv. Synth. Catal. 353 (2011) 1897-1902.
[50] M. C. Holz, K. Toelle, M. Muhler, Catal. Sci. Technol. 4 (2014) 3495-3504.
[51] A. Abad, P. Conceptcion, A. Corma, H. Garcia, Angew. Chem. Int. Ed. 44 (2005) 4066-4069.
[52] A. Abad, C. Almela, A. Corma, H. Garcia, Tetrahedron 62 (2006) 6666-6672.
[53] H. Tsunoyama, H. Sajurai, Y. Negishi, T. Tsukuda, J. Am. Chem. Soc. 127 (2005) 9374-9375.
[54] F. Z. Su, Y. M. Liu, L. C. Wang, Y. Cao, H. Y. He, K. N. Fan, Angew. Chem. Int.Ed. 47 (2008) 334-337.
[55] L. C. Wang, L. He, Q. Liu, Y. M. Liu, M. Chen, Y. Cao, H. Y. He, K. N. Fan, Appl. Catal. A. 344 (2008) 150-157.
[56] L. C. Wang, Y. M. Liu, M. Chen, Y. Cao, H. Y. He, K. N. Fan, J. Phys. Chem. C. 11 (2008) 6981-6987.
[57] J. F. Gohy, N. Willet, S. Varshney, J. X.Zhang, R. J éröme, Angew. Chem. Int. Ed. 40

(2001) 3214-3216.
[58] L. Lei, J. F. Gohy, N. Willet, J. X. Zhang, S. Varshney, R. Jéröme, Macromolecules 37 (2004) 1089-1094.
[59] A. Khanal, Y. Li, N. Takisawa, N. Kawasaki, Y. Oishi, K. Nakashima, Langmuir 20 (2004) 4809-4812
[60] A. Khanal, K. Nakashima, N. Kawasaki, Y. Oishi, M. Uehara, H. Nakamura, Y. Tajima, Colloid Polym. Sci. 283 (2005) 1226-1229.
[61] M. Sasidharan, D. Liu, N. Gunawardhana, M. Yoshio, K. Nakashima, J. Mater. Chem. 21 (2011) 13881-13888.
[62] M. Kanehara, E. Kodzuka, T. Teranishi, J. Am. Chem. Soc. 128 (2006) 13084-13094
[63] C. H. Shi, N. W. Zhu, Y. L. Cao, P. X. Wu, Nanoscale Res. Lett. 10 (2015) 147-154.
[64] M. Sasidharan, A. Bhaumik, J. Mol. Catal. A: Chem. 328 (2010) 60-67
[65] T. Wang, C. X. Xiao, L. Yan, L. Xu, J. Luo, H. Shou, Y. Kou, H. C. Liu, Chem. Commun. (2007) 4375-4376.
[66] G. ten Brink, I. W. C. E. Arends, R. A. Sheldon, Science 287 (2000) 1636-1639.
[67] X. Wang, H. Kawanami, N. M. Islam, M. Chatterjee, T. Yokoyama, Y. Ikushima, Chem. Commun. (2008) 4442-4443
[68] B. K. Pong, H. I. Elim, J. X. Chong, W. Ji, B. L. Trout, J. Y. Lee, J. Phys. Chem. C 111 (2007) 6281-6287.
[69] A. Abad, A. Coma, H. Garcia, Chem. Eur. J. 14 (2008) 212-222.
[70] J. Ni, W-J. Yu, L. He, H. Sun, Y. Cao, H-Y. He, K. N. Fan, Green Chem. 11 (2009) 756-759

Figure captions:

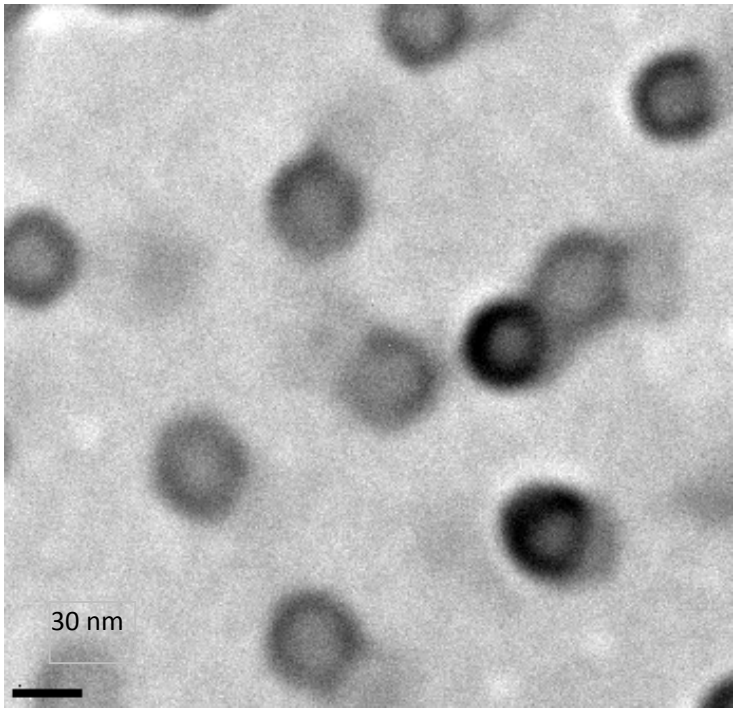

Figure 1. TEM image of PS-PVP-PEO micelles.

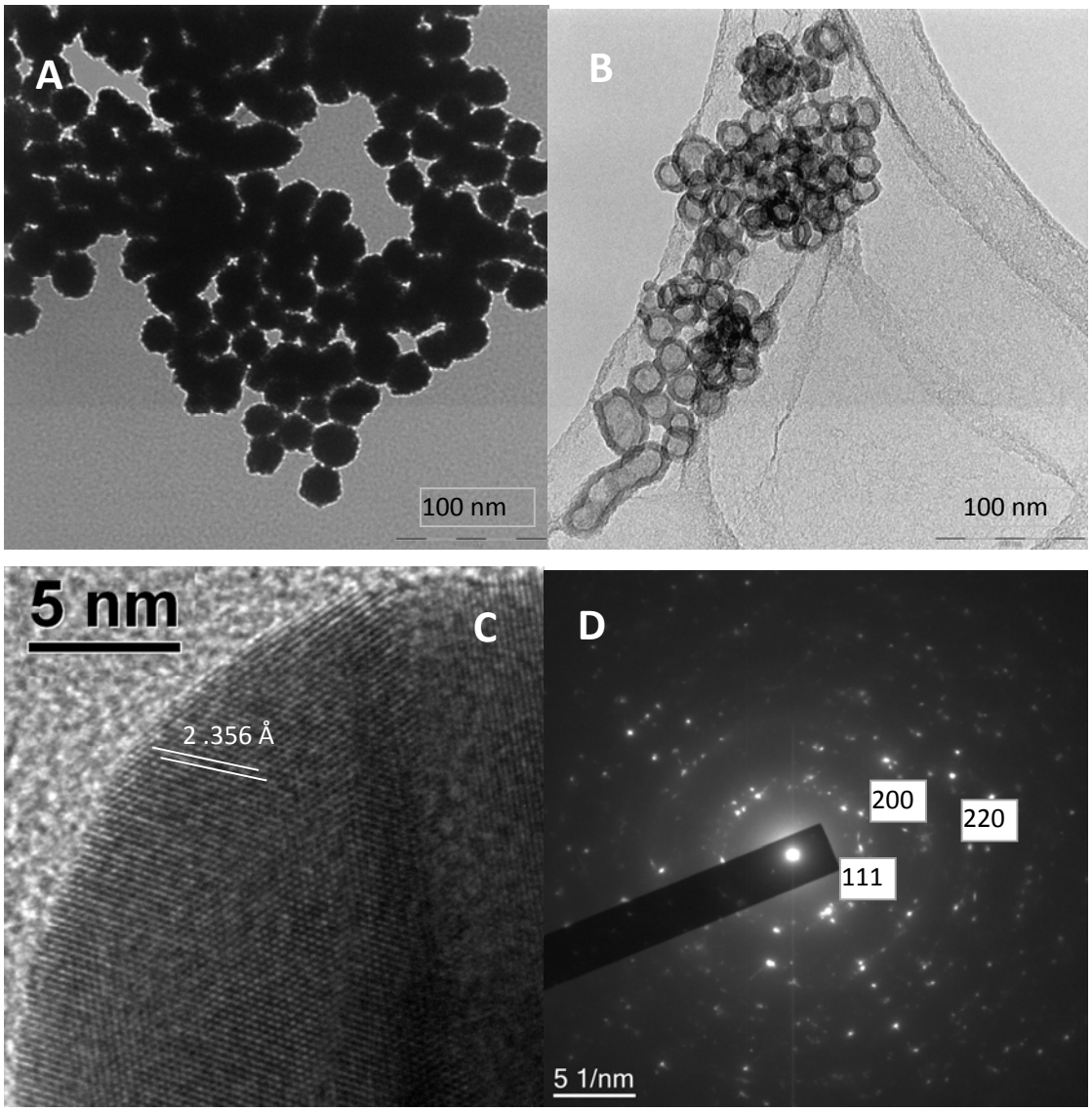

Figure 2. TEM images of (A) Au/polymer composite particles; (B) Au hollow nanospheres; (C) High resolution TEM of Au hollow nanospheres; and (D) Electron diffraction pattern.

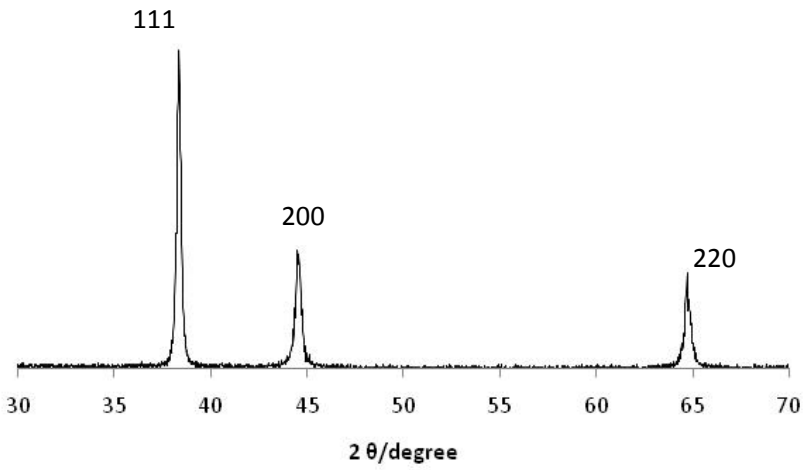

Figure 3. X-ray diffraction pattern of Au hollow nanospheres.

Scheme 1

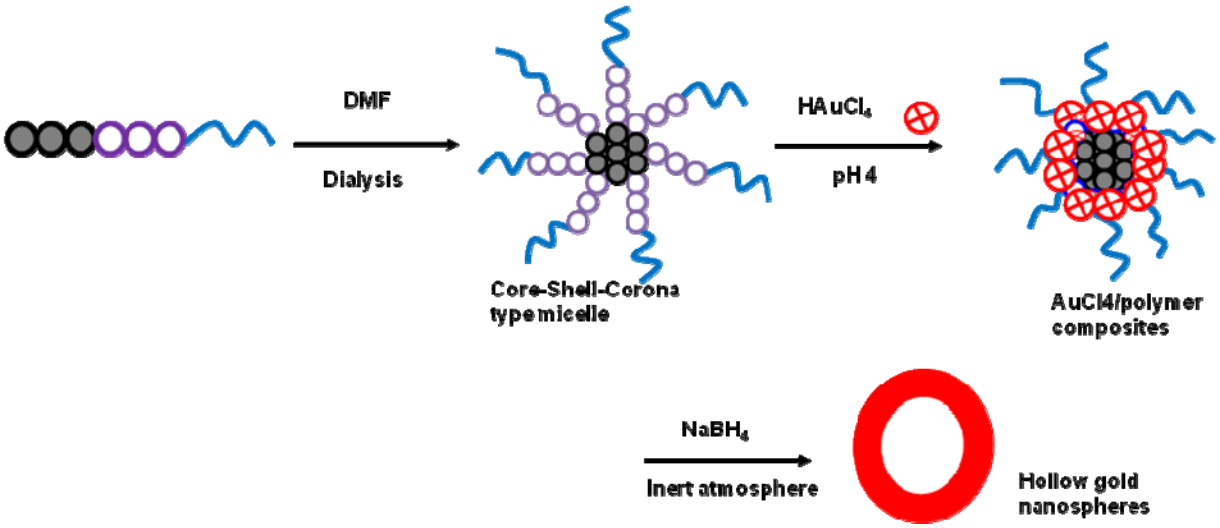

Scheme 2

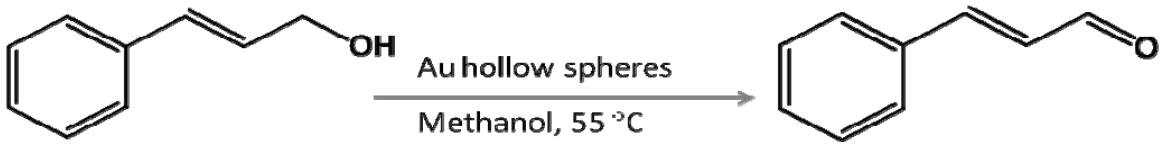

Table 1: Influence of solvents and catalyst loading over selective oxidation of cinnamyl alcohol using Au/H_2O_2 system[a]

Entry	Solvents	Conversion, (mol %)	Selectivity,%
1	Acetonitrile	93.2	98.8
2	Methanol	98.2	100
3	Ethanol	97.8	100
4	Dichloromethane	71.9	100
5	Nitromethane	82.8	98.9
6	Ethylacetate	94.8	97.6
7	Toluene	94.7	98.2
8[b]	Methanol	98.5	99.8
9[c]	Methanol	79.5	99.6

[a]Reaction conditions: 5 mmol substrate, 5 mmol H_2O_2, 10 mL solvent, 5 wt% catalysts; 0.1 mmol cycloheptanone as internal standard, temperature 55 °C, reaction time 8 h; [b]10 wt % catalysts; [c] 3 wt % catalysts used.

Table 2. Chemoselective oxidation of different alcohols using Au hollow nanospheres/H_2O_2 catalytic system[a]

Entry	Substrate	Product	Conversion, (mol %)	Selectivity,%
1	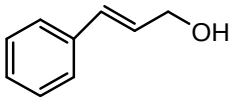	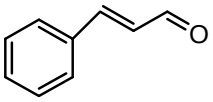	98.2	100
2	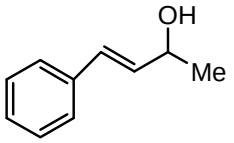	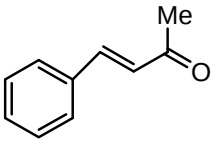	98.5	100
3	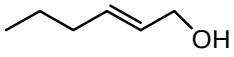	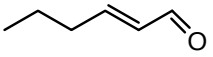	97.6	99.4
4	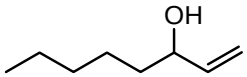	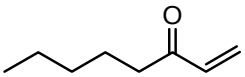	98.3	99.2
5	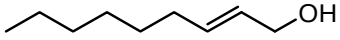	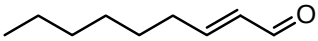	98.9	94.3[b]
6	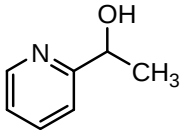	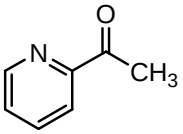	95.8	99.0
7	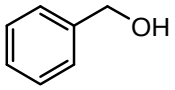	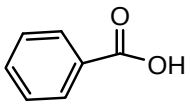	99.0	87.0[b]
8	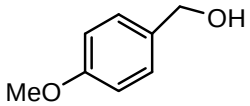	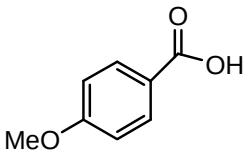	98.6	66.0[b]
9	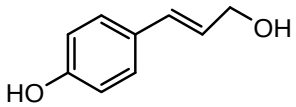	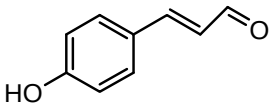	96.4	99.3
10	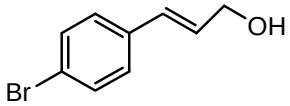	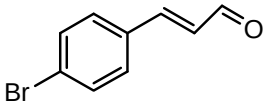	70.9	99.0
11	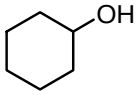	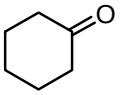	91.0	99.1
12	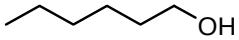	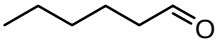	97.8	89.5[c]
13[d]	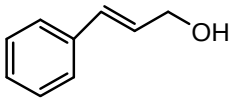	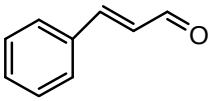	trace	-
14[e]	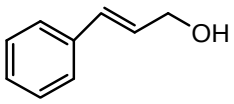	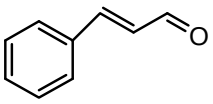	94.4	99.2

15[f]	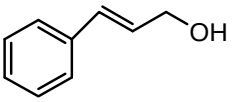	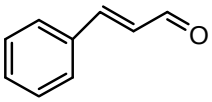	72.9	99.1

[a]Reaction conditions: 5 mmol substrate, 5 mmol H_2O_2, 10 mL methanol, 5 wt % catalyst used, 0.1 mmol cycloheptanone as internal standard, temperature 55 °C, reaction time 8 h; [b]Aldehyde; [c]Carboxylic acid; [d] No catalyst was used; [e] The catalyst was reused 4 times successively; [f]Au spherical particles of size 20-30 nm prepared by using sodium citrate reducing agents.